Max Planck Institute Magdeburg
Preprints

Peter Benner Lihong Feng

Model Order Reduction for Coupled Problems

MPIMD/15-02 **February 13, 2015**

Imprint:

Max Planck Institute for Dynamics of Complex Technical Systems, Magdeburg

Publisher:
Max Planck Institute for
Dynamics of Complex Technical Systems

Address:
Max Planck Institute for
Dynamics of Complex Technical Systems
Sandtorstr. 1
39106 Magdeburg

http://www.mpi-magdeburg.mpg.de/preprints/

Abstract

In this survey, we provide an overview of model order reduction (MOR) methods applied to coupled systems. The coupling can be linear or nonlinear, weak or strong. Physically, the coupling may come from structure-structure coupling, fluid-structure or fluid-fluid interaction, electro-thermal coupling, electro- or thermal-mechanical coupling, or circuit-device coupling. Different MOR methods for coupled systems are reviewed, and numerous examples of coupled systems from the open literature are used for illustration.

Keywords: model order reduction, coupled problems, multi-physics, numerical methods.

AMS Subject Classification: 34K17, 74F05, 74F10, 93A15, 93B40.

1 Introduction

Coupled systems exist in many engineering applications, in particular in multi-physics problems. The coupling is caused by interaction between different subsystems, describing different physical quantities, such as temperature, structural mechanical displacements, electro-magnetic fields, and so forth. The interaction usually takes place inside a domain of interest or through the boundary of the domain of interest. After numerical discretization of the mathematical models of the coupled systems, the discretized systems are usually complex and of very large scale. This has motivated the application of model order reduction techniques, intending to reduce the number of degrees of freedom, enable practical computation, and furthermore, significantly reduce the computational time.

Model order reduction for coupled systems has been studied in structural dynamics since the 1960s [14], where a component mode synthesis (CMS) method was proposed. An overview of CMS methods can be found in [8]. In [23], the problem how to choose the important modes of the subsystems within CMS methods is addressed, and a moment-matching approach for choosing important modes is proposed. The CMS method builds upon the modal truncation method [9] known in control and mechanical engineering, and in this sense, CMS belongs to modal truncation methods [16].

Besides the CMS method widely used in structural dynamics [8, 30], MOR methods based on systems and control theory like balanced truncation [32, 6, 28, 29, 19], and MOR methods based on approximation theory like moment-matching [33, 15, 24, 34, 19, 5], as well as the MOR methods popular in mechanical engineering and fluid dynamics like the reduced basis method [25, 27], proper orthogonal decomposition (POD) [20, 13], have been subsequently applied to coupled systems, and have achieved significant efficiency for various multi-physics problems. In the following sections, we review all the above MOR methods according to the coupled systems considered. We go through linear and nonlinear coupled systems. In each class, systems consisting of different physical couplings are addressed.

2 Coupled systems: a general description

The linear coupled systems considered in this report are either in the first-order form

$$\begin{aligned} \underbrace{\begin{bmatrix} E_{11} & \dots & E_{1k} \\ \vdots & \ddots & \vdots \\ E_{k1} & \dots & E_{kk} \end{bmatrix}}_{\mathcal{E}} \begin{bmatrix} \dot{x}_1 \\ \vdots \\ \dot{x}_k \end{bmatrix} &= \underbrace{\begin{bmatrix} A_{11} & \dots & A_{1k} \\ \vdots & \ddots & \vdots \\ A_{k1} & \dots & A_{kk} \end{bmatrix}}_{\mathcal{A}} \begin{bmatrix} x_1 \\ \vdots \\ x_k \end{bmatrix} + \begin{bmatrix} B_1 \\ \vdots \\ B_k \end{bmatrix} u, \\ y &= [C_1^T, \dots, C_k^T] \begin{bmatrix} x_1 \\ \vdots \\ x_k \end{bmatrix}, \end{aligned} \tag{1}$$

or in the second-order form

$$\begin{aligned} \underbrace{\begin{bmatrix} M_{11} & \dots & M_{1k} \\ \vdots & \ddots & \vdots \\ M_{k1} & \dots & M_{kk} \end{bmatrix}}_{\mathcal{M}} \begin{bmatrix} \ddot{x}_1 \\ \vdots \\ \ddot{x}_k \end{bmatrix} + \mathcal{E} \begin{bmatrix} \dot{x}_1 \\ \vdots \\ \dot{x}_k \end{bmatrix} + \mathcal{A} \begin{bmatrix} x_1 \\ \vdots \\ x_k \end{bmatrix} &= \begin{bmatrix} B_1 \\ \vdots \\ B_k \end{bmatrix} u, \\ y &= [C_1^T, \dots, C_k^T] \begin{bmatrix} x_1 \\ \vdots \\ x_k \end{bmatrix}. \end{aligned} \tag{2}$$

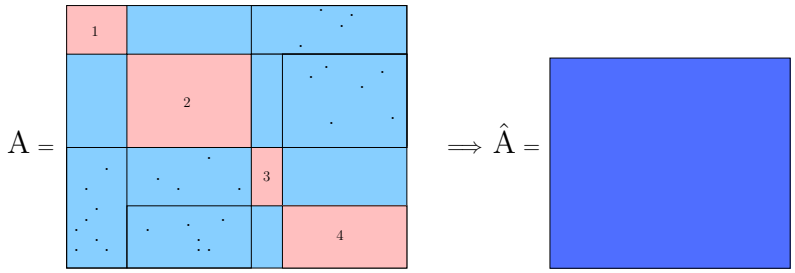

Figure 1: Classical MOR: block structure is lost.

Here $E_{ij}, A_{ij}, M_{ij} \in \mathbb{R}^{n_i \times n_j}$, $B_i \in \mathbb{R}^{n_i \times p_i}, C_i \in \mathbb{R}^{n_i \times m_i}$. Each of the state vectors $x_i \in \mathbb{R}^{n_i}$, $i, j = 1, \ldots, k$, is the state vector of the ith subsystem. For the state matrices of the fully coupled system, we have $\mathcal{M}, \mathcal{E}, \mathcal{A} \in \mathbb{R}^{n \times n}$ with $n = n_1 + \ldots + n_k$.

Usually there are some zero-blocks in the matrices $\mathcal{M}$, $\mathcal{E}$ and $\mathcal{A}$, i.e. $E_{ij} = 0, A_{ij} = 0, or M_{ij} = 0$ for certain i, j. This is due to the fact that two of the subsystems are not coupled or the coupling holds only in one direction (one way coupling) [24]. For nonlinear coupled systems, nonlinear functions of the state vectors x_i will appear in the system, see e.g., the examples in Section 5.

It is always desired, either from a numerical point of view, or from a physical point of view, that the block structure of the coupled system should be preserved in the reduced-order model. Hence, MOR for coupled systems usually follows this basic principle. In the sequel, we first introduce the general idea of structure preserving MOR, then we present typical examples of the coupled systems, and introduce MOR methods that are tailored for each case.

3 Block structure preserving MOR for coupled systems

3.1 Standard BSP MOR methods.

Block structure preserving (BSP) MOR for linear coupled systems, in the above general form (1), is discussed in [34, 24], where the block structures of the coupled systems are preserved. More specifically, the zero-block matrices in the coupled system remain zero-blocks after MOR. For classical MOR methods, the resulting system matrices in the reduced-order model are usually dense, as is shown in Figure 1. However, if using block structure preserving MOR, the resulting system matrices, e.g., $\hat{A}$ in the reduced-order model, preserve the block structure of the original matrix A, as can be seen from Figure 2. There we can see that at least the zero-blocks in A are preserved as zero-blocks in $\hat{A}$. In both figures, the empty off-diagonal blocks in A and $\hat{A}$ represent the zero-block matrices.

The basic idea of *standard* BSP MOR is that instead of using the projection matrices W, V (e.g., computed from the classical balanced truncation method [1], moment-matching [12, 11], or any other projection method) directly, W, V are divided into k blocks (note that there are k subsystems),

$$W = \begin{bmatrix} W_1 \\ \vdots \\ W_k \end{bmatrix}, \quad V = \begin{bmatrix} V_1 \\ \vdots \\ V_k \end{bmatrix}.$$

Next, the blocks W_i, V_i are used to construct the structure preserving projection matrices

$$\tilde{W} = \begin{bmatrix} W_1 & & \\ & \ddots & \\ & & W_k \end{bmatrix}, \quad \tilde{V} = \begin{bmatrix} V_1 & & \\ & \ddots & \\ & & V_k \end{bmatrix}, \tag{3}$$

The reduced-order model obtained by using $\tilde{W}$ and $\tilde{V}$ instead of W and V preserves the block structure of the original coupled system. It should be pointed out that the above *standard* BSP MOR method does not represent all the BSP MOR methods to be introduced in the following sections. Many BSP MOR methods can directly compute W_i and V_i, instead of getting them from W, V computed by classical MOR methods. Here, we first introduce a "separate bases reduction" method from [24], which directly computes W_i and V_i for MOR of the system in the general form in (1).

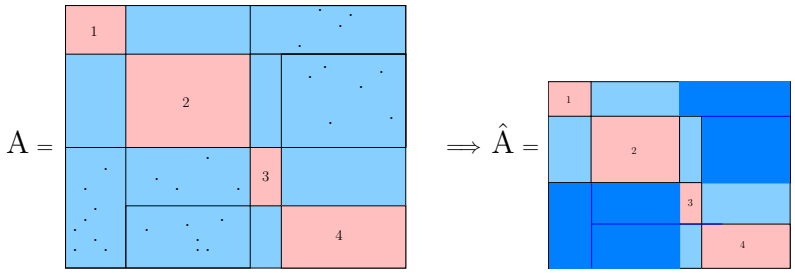

Figure 2: BSP MOR: block structure is preserved.

3.2 Separate bases reduction (SBR) method

The linear coupled system in (1) is considered in [24] for MOR. The method is slightly different from the above introduced standard BSP method. The main difference is that the process of constructing the block matrices V_i and W_i in (3) is reordered. In the standard BSP method, the projection matrices W, V are firstly computed using, e.g., the classical moment-matching method, and then divided into blocks W_i and V_i. In the SBR method, each matrix pair W_i and V_i is first computed for each subsystem, using the moment-matching method [12]. Then they are put together to constitute the block-wise projection matrices $\tilde{W}, \tilde{V}$ in (3). When using the moment-matching method, the coupling blocks in each subsystem are considered as inputs for the current subsystem. That is, for the current jth subsystem, the matrix R in the Krylov subspace $\mathcal{K}_r(A, R)$ includes both the input matrix B_j and the coupling matrix A_{ji}, e.g., $R = [B_j, A_{ji}]$, where $A_{ji} \neq 0$, for $i \neq j$, is the coupling between the current subsystem (jth subsystem) and the ith subsystem (see Chapter 5 and Chapter 8 in [24]). The advantage of the SBR method over the standard BSP method for MOR of coupled systems is that its computational cost and storage requirements are much lower.

For different application backgrounds, the coupling of the systems is different. In most cases, the number of subsystems is small. Usually, there are 2 to 3 subsystems in a coupled system, i.e. $k = 2, 3$ in (1) or (2). In the following we classify them according to the linearity of the coupling. Several examples of coupled systems are presented and the proper MOR methods for each kind of coupled systems are introduced. If feasible, the partial differential equations of the mathematical models are also provided.

4 MOR for linear coupled systems

4.1 Coupling through internal states

In most coupled systems, the coupling is through the state variables of the system. In this subsection, we introduce MOR for linear coupled systems that are coupled through the state variables. We study typical cases with electro-mechanical coupling, thermal-elastic coupling, and flow coupling through an interface.

4.1.1 A model of an adaptive spindle support

The piezo-mechanical model shown in Figure 3 and Figure 4, is a complex system, where a piezo-actuator based adaptive spindle support (ASS) is mounted on a parallel kinematic test machine [26]. Based on the engineering design with a differential setup of the piezo stack actuators, the suitability for a special application is mainly defined by the applied control concept. Before being implemented in the real machine, system simulation is needed to design and test the control concept.

Applying the finite element method (FEM) to the ASS shown in Figure 5 leads to a mathematical model of the following form:

$$\begin{aligned} M\ddot{x}(t) + E\dot{x}(t) + Kx(t) &= Bu(t), \\ y(t) &= C_1\dot{x}(t) + C_2x(t) + Du(t), \end{aligned} \tag{4}$$

where M, E and $K \in \mathbb{R}^{n\times n}$ are the sparse FEM-matrices resulting from the modeling, $B \in \mathbb{R}^{n\times p}$ is the input matrix describing the external access to the system, and $C_1, C_2 \in \mathbb{R}^{m\times n}$ represent the measurements. Accordingly, $u(t) \in \mathbb{R}^p$ and $y(t) \in \mathbb{R}^m$ are the control inputs to the system and the measured outputs, respectively, $D \in \mathbb{R}^{m\times p}$ represents the direct feed through from input to the output.

In the special case of the piezo mechanical system, $x = (v^T, \Phi^T)^T$, where v represents the mechanical displacements and Φ the electrical potentials at the piezo actuators. Therefore the system matrices take the special form [17]

$$M = \begin{bmatrix} M_{vv} & 0 \\ 0 & 0 \end{bmatrix}, \quad E = \begin{bmatrix} E_{vv} & 0 \\ 0 & 0 \end{bmatrix}, \quad K = \begin{bmatrix} K_{vv} & K_{v\Phi} \\ K_{v\Phi}^T & K_{\Phi\Phi} \end{bmatrix}, \tag{5}$$

where the mass matrix M has rank deficiency. The matrix $K_{v\Phi}$ describes the coupling between v and Φ. Simulation with the finite element model is not feasible due to the large number of degrees of freedom.

MOR for the spindle support model

In [32], the authors obtained a first-order reduced state space model in order to facilitate fast simulation using MATLAB® Simulink. The basic steps are firstly transforming the second order system into a first order system, then using the balanced truncation method to get a first order reduced-order model. The reduced-order model can be used in MATLAB Simulink. If otherwise, one wants to obtain a reduced second order model that preserves the structure of the original model to perform the simulation work using special software (if it is necessary), it is also not difficult to get a reduced-order model in the second order form, see [6]. In [6], the balanced truncation method [1] is applied to get the reduced-order model. To preserve the structure of the original system, the full Gramians are replaced by the corresponding combination of position and velocity Gramians during the model order reduction procedure.

4.1.2 A thermo-elastic model

In many machine production applications one has to deal with thermally driven deformations of the machine tools and the workpieces to be processed. In order to compensate, e.g., production inaccuracies, one needs to forecast the thermo-elastic behavior of the procedure. Since the time scale of the elastic behavior is much smaller than that of the heat model, it is sufficient to assume that the temperature field is not affected by the deformations. Therefore, in the following we consider a one-way coupling of the resulting thermo-elastic system. Furthermore, the treatment of a stationary linear elasticity model leads to satisfactory results as long as the deformations are mainly caused by thermal influences. The temperature evolution is modeled by the partial differential equation (PDE)

$$c_p \rho \dot{T} = \operatorname{div}(\lambda \nabla T), \qquad \text{on } \Omega, \tag{6a}$$

$$\lambda \frac{\partial}{\partial n} T = z_{th}, \qquad \text{on } \Gamma \subset \partial\Omega, \tag{6b}$$

$$T(t_0) = T_0, \tag{6c}$$

with T defining the temperature field, z_{th} describing external temperature inputs of the system and c_p, ρ, λ are the material parameters, namely the specific heat capacity, density and heat conductivity, respectively. Note that there is no explicit influence of the associated displacement field. Moreover, as mentioned above, the deformation u acts much faster than the underlying temperature field. Hence it is sufficient to model the elastic behavior by a

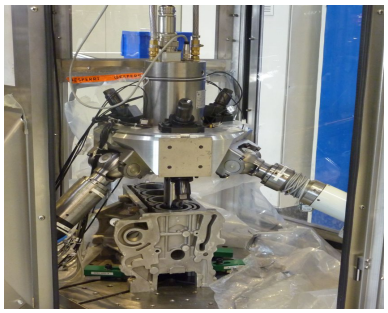

Figure 3: Piezo-actuator based mechanical system. (Courtesy of Fraunhofer IWU, Dresden.)

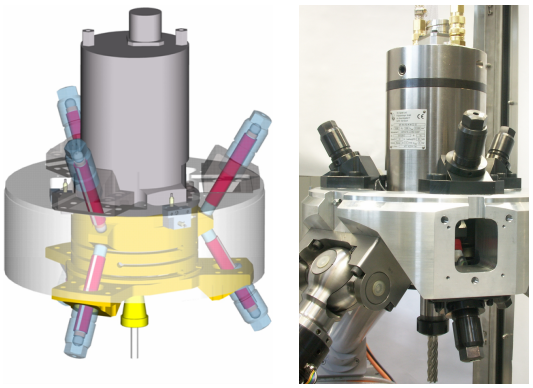

Figure 4: The adaptive spindle support: CAD-model (left) and real component mounted on the test bench (right). (Courtesy of Fraunhofer IWU, Dresden.)

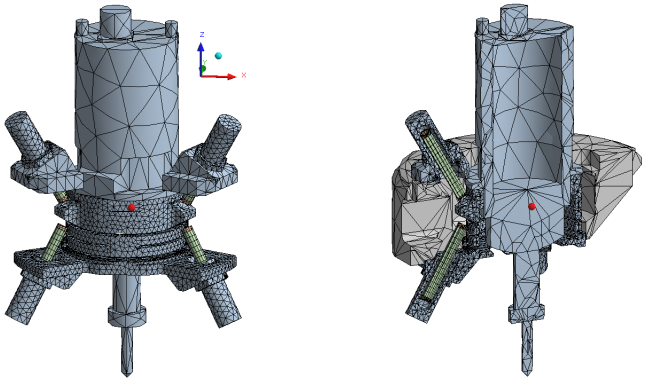

Figure 5: Details of the finite element mesh of the adaptive spindle support. (Courtesy of Fraunhofer IWU, Dresden.)

stationary linear PDE of the form

$$
\begin{aligned}
-\operatorname{div}(\sigma(u)) &= f, && \text{on } \Omega, && \text{(7a)}\\
\varepsilon(u) &= \mathbf{C}^{-1} : \sigma(u) + \beta(T - T_{ref})I_d, && \text{on } \Omega, && \text{(7b)}\\
\mathbf{C}^{-1}\sigma(u) &= \frac{1+\nu}{E_u}\sigma(u) - \frac{\nu}{E_u}\operatorname{tr}(\sigma(u))I_d, && \text{on } \Omega, && \text{(7c)}\\
\varepsilon(u) &= \frac{1}{2}(\nabla u + \nabla u^T), && \text{on } \Omega, && \text{(7d)}
\end{aligned}
$$

where σ denotes the mechanical stress and ε is the strain of the domain Ω. The coefficients E_u, ν, β describe Young's modulus, Poisson's ratio and the thermal expansion coefficient, respectively. Further elastic deformations induced by external body forces are incorporated by the elasticity inputs z_{el}. In order to allow us to use the linear stationary elasticity equations, the elasticity inputs are assumed to be small and changes of these inputs are slow. The expression $\mathbf{C}$ denotes the stiffness tensor, which is a fourth order tensor and I_d is the identity of size d which is the spatial dimension of Ω. For further details on the continuum mechanics based modeling of elasticity phenomena, we refer to [10]. The above mentioned coupling of the thermal and elastic model is given by the thermally induced strain

$$\beta(T - T_{ref})I_d,$$

stated in equation (7b). This indicates that the resulting displacement is induced by the change of temperature T with respect to a given reference temperature T_{ref} of Ω at time t_0.

Discretizing equations (6) and (7) by e.g., the finite element method (FEM), we obtain

$$\begin{aligned} E_{th}\dot{T}(t) &= A_{th}(t)T(t) + B_{th}(t)z_{th}(t), \\ 0 &= A_{thel}T(t) - A_{el}u(t) + B_{el}z_{el}(t), \\ T(t_0) &= T_0, \quad u(t_0) = 0, \end{aligned} \tag{8}$$

where $E_{th}, A_{th} \in \mathbb{R}^{\tilde{n}\times\tilde{n}}$, $B_{th} \in \mathbb{R}^{\tilde{n}\times p_{th}}$, $A_{thel} \in \mathbb{R}^{3\tilde{n}\times\tilde{n}}$, $A_{el} \in \mathbb{R}^{3\tilde{n}\times 3\tilde{n}}$ and $B_{el} \in \mathbb{R}^{3\tilde{n}\times p_{el}}$, $\tilde{n}$ denotes the number of nodes of the underlying FE grid, and p_{th}, p_{el} are the numbers of thermal and elasticity inputs, respectively. That is, we consider $\tilde{n}$ temperature degrees of freedom (DOFs) and additionally $3\tilde{n}$ elasticity DOFs corresponding to the deformations in the three spatial dimensions. The system (8) can be re-written into the coupled thermo-elastic system

$$\begin{aligned} \begin{bmatrix} E_{th} & 0 \\ 0 & 0 \end{bmatrix} \begin{bmatrix} \dot{T} \\ \dot{u} \end{bmatrix} &= \begin{bmatrix} A_{th} & 0 \\ A_{thel} & -A_{el} \end{bmatrix} \begin{bmatrix} T \\ u \end{bmatrix} + \begin{bmatrix} B_{th} & 0 \\ 0 & B_{el} \end{bmatrix} \begin{bmatrix} z_{th}(t) \\ z_{el}(t) \end{bmatrix}, \\ \begin{bmatrix} T(t_0) \\ u(t_0) \end{bmatrix} &= \begin{bmatrix} T_0 \\ 0 \end{bmatrix}. \end{aligned} \tag{9}$$

Due to the one-way coupling and the consequential particular structure, equation (9) is a system of differential-algebraic equations (DAE) of index 1. It is a generalized state-space or descriptor system. Furthermore, we add an output equation

$$y(t) = [0, C_{el}] \begin{bmatrix} T \\ u \end{bmatrix} \tag{10}$$

to observe certain degrees of freedom of interest. Here, $C_{el} \in \mathbb{R}^{m\times 3\tilde{n}}$ filters out the interesting deformation information.

MOR for coupled thermo-elastic systems

Model order reduction (MOR) for the descriptor system in (9) and (10) has been studied in the literature, see e.g., [12, 11, 31] and the references therein. However, these methods do not take the special structure of the system into consideration, and therefore destroy the block structure of the system. In fact, the block structure arising from the one-sided coupling of the thermal and elasticity model in (9) can be exploited. The application of the Schur complement as proposed in [11] to the DAE yields an equivalent system

$$\begin{aligned} E_{th}\dot{T} &= A_{th}T(t) + B_{th}z(t), \\ y &= C_{el}A_{el}^{-1}A_{thel}T + C_{el}A_{el}^{-1}B_{el}z_{el}(t) =: \tilde{C}T + \tilde{D}z_{el}(t), \end{aligned} \tag{11}$$

which relies on the dimension $\tilde{n}$ of the thermal model. Note that after the application of the Schur complement to the one-sided coupled thermo-elastic system, all the information of the stationary elasticity model is captured by the modified output $\tilde{C}$. Using the Schur complement, the given one-sided coupled DAE system (9) of dimension $n = 4\tilde{n}$ together with the output equation (10) can be equivalently reformulated into a system of the form (11). Thus, any MOR method can be applied to a system of dimension $\tilde{n}$ instead of $4\tilde{n}$ with a modified output $\tilde{C}$, which contains the entire information of the elasticity model.

Now, the problem can easily be stated as a standard state-space linear time-invariant system, since the FE mass matrix E_{th} of the thermal model is non-singular, and the classical MOR methods as mentioned above can be applied to the standard-state-space system in (11). In [19], a coupled thermo-elastic system of the form (9), where $B_{el} = 0$ and additionally the matrices A_{th}, B_{th} vary with respect to a moving thermal load, is treated by MOR. The variation of the matrices A_{th}, B_{th} is modeled via two different approaches. The first approach uses switched linear systems (SLS) to capture the movement. Then balanced truncation method is used to reduce each of the linear systems in the SLS. A speedup factor of 62 has been achieved by the reduced-order models. The original SLS have the same dimension $n = 16,626$, and the reduced-order models are all of size 60. The second approach handles the variability of the model via a parameter describing the moving load which results in a parametric coupled system with dimension $n = 16,626$. In this case the iterative rational Krylov algorithm (IRKA) [3] is applied to compute a reduced-order model with size 75, which has resulted in a speedup factor of 584.

4.1.3 A coupled Stokes-Darcy system

In [25], a coupled Stokes-Darcy system is considered. It is coupling of a free flow with a flow through porous media. The computational domain Ω is decomposed into two sub-domains Ω_1 and Ω_2, as is illustrated in Figure 6, where Γ is the interface, with associated normal unit vector $\mathbf{n}$ pointing from Ω_1 to Ω_2 and tangent with unit vector τ. The mathematical model in the PDE form is as follows. On Ω_1, a Stokes flow is considered: find velocity $\mathbf{u}$ and

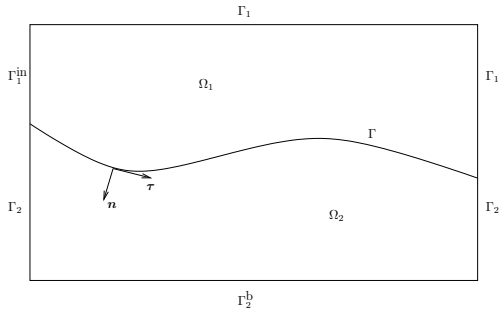

Figure 6: Illustration of the computational domains and boundaries for the coupled Stokes-Darcy system.

pressure p such that

$$\begin{array}{rcll} -\nu\Delta\mathbf{u}+\nabla p &=& \mathbf{f} & \text{in } \Omega_1, \\ \Delta\cdot\mathbf{u} &=& 0 & \text{in } \Omega_1, \\ \mathbf{u} &=& \mathbf{u}_{in} & \text{on } \Gamma_1^{in} \\ \mathbf{u} &=& 0 & \text{on } \Gamma_1, \end{array} \tag{12}$$

and on Ω_2, the porous media equation is considered:

$$\begin{array}{rcll} -\Delta\cdot(K\nabla\phi) &=& 0 & \text{in } \Omega_2, \\ -K\nabla\phi\cdot\mathbf{n}_2 &=& 0 & \text{in } \Gamma_2, \\ \phi &=& \phi_b & \text{on}\Gamma_2^b. \end{array} \tag{13}$$

The two systems above are coupled though the following interface conditions on Γ:

$$\begin{array}{rcll} \mathbf{u}\cdot\mathbf{n} &=& -\frac{1}{n}K\nabla\phi\cdot\mathbf{n} & \text{on } \Gamma, \\ -\nu\mathbf{n}\cdot\frac{\partial\mathbf{u}}{\partial\mathbf{n}}+p &=& g\phi & \text{on } \Gamma, \\ \mathbf{u}\cdot\tau &=& -\frac{\sqrt{k}}{\alpha_{BJ}}\tau\cdot\frac{\partial\mathbf{u}}{\partial\mathbf{n}} & \text{on } \Gamma. \end{array} \tag{14}$$

MOR for Stokes-Darcy system.

The reduced basis method is used to compute the projection matrices for MOR in [25]. The projection matrices V_u and V_p for the velocity $\mathbf{u}$ and the pressure p, as well as the projection matrix V_ϕ for ϕ, are computed separately using a greedy algorithm, where the coupling was considered when computing the reduced basis. The reduced-order model is derived by using Galerkin projection, applying V_u, V_p, and V_ϕ, respectively, to the discretized version of the model in (12)–(14). The details can be found in [25], where as a convention in the reduced basis community, the discretized system is not explicitly presented. All the analyses are done in the operator form, and in functional space. Compared to full simulation of the original large model, the online simulation of the reduced-order model with relative error 6.72×10^{-4}, has achieved a speed-up factor of 877. The offline time of generating the reduced-order model is reported to be around 3 hours. After discretization in space, the dimension of the original coupled system is $n = 92,168$, and that of the reduced-order model is 171.

4.1.4 An acoustic cavity model

In [30], a cube-shaped acoustic cavity filled with air or water is considered for simulation and model order reduction. The geometric model and its discretization are depicted in Figure 7. The model is constructed with a linear description of vibro-acoustics phenomena based on a displacement-pressure formulation. The behavior of the structure-fluid undamped coupled system is described by the following equations after finite element discretization,

$$\begin{bmatrix} M_s & 0 \\ \rho_f C^T & M_f \end{bmatrix}\begin{pmatrix} \ddot{u} \\ \ddot{p} \end{pmatrix}+\begin{bmatrix} K_s & -C \\ 0 & K_f \end{bmatrix}\begin{pmatrix} u \\ p \end{pmatrix}=\begin{pmatrix} F_s \\ 0 \end{pmatrix}, \tag{15}$$

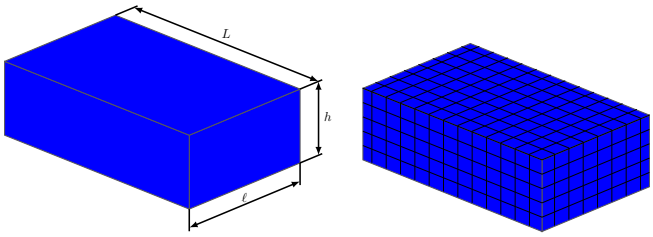

Figure 7: Geometry (a) and its discretization (b) of the acoustic cavity model.

where $M_s \in \mathbb{R}^{n_s \times n_s}, K_s \in \mathbb{R}^{n_s \times n_s}, C \in \mathbb{R}^{n_s \times n_f}, M_f \in \mathbb{R}^{n_f \times n_f}, K_f \in \mathbb{R}^{n_f \times n_f}$. In the system above, the equation for the displacement u includes the contribution of the pressure p, and the equation for the pressure p includes the derivatives of u with respect to time t. The coupling occurs in both equations, so that it is a two-way coupling, or in other words it is a strong coupling problem.

MOR for the acoustic cavity model

The classical model order reduction technique in structural dynamics is to use the eigenmodes of the uncoupled structure and fluid systems to construct the projection matrix for MOR. More specifically, the uncoupled eigenvalue problems

$$\begin{array}{rcl} (-\omega^2 M_s + K_s)U &=& 0, \\ (-\omega^2 M_f + K_f)P &=& 0 \end{array} \tag{16}$$

are solved to get the eigenmodes of the structure and fluid systems $V_{s_0} \in \mathbb{R}^{n_s \times r_s}$, and $V_{f_0} \in \mathbb{R}^{n_f \times r_f}$, $r_s \ll n_s, r_f \ll n_f$. The reduced-order model is constructed by Galerkin projection with the projection matrix $V = \text{diag}\{V_{s_0}, V_{f_0}\}$, i.e., V_{s_0}, and V_{f_0} are the two diagonal blocks of V. The system matrices of the reduced-order model are then constructed as:

$$\hat{K}_s = V_{s_0}^T K_s V_{s_0}, \hat{M}_s = V_{s_0}^T M_s V_{s_0}, \hat{C} = V_{s_0}^T K_s V_{f_0}, \hat{F}_s = V_{s_0}^T F_s, \hat{K}_f = V_{f_0}^T K_f V_{f_0}, \hat{M}_f = V_{f_0}^T M_f V_{f_0}.$$

The classical model order reduction technique as above simply ignores the effect of the coupled modes, which may lead to a very low accuracy. Further improved methods are proposed, see e.g., the detailed description in [30]. All the improved methods try to include the influence of the coupled modes into the projection matrix V, i.e., into the reduced bases, by using different techniques. The methods of using some of the important eigenmodes of the system to construct the reduced-order model are usually called modal truncation methods in mechanical engineering, or component mode synthesis methods (CMS) [8] in structural dynamics. It is reported in [30] that the simulation time of solving the reduced-order model obtained by the classical MOR method of using eigenmodes of the uncoupled systems is only 1 percent of that spent on solving the original coupled system. Although the improved MOR methods proposed in [30] produce more accurate results, they only bring a speedup factor of 2 as compared to direct simulating the full coupled system.

4.2 Coupling through inputs and outputs: interconnected systems

In this section, we introduce MOR methods for systems coupled through internal inputs and internal outputs [28, 33].

4.2.1 Model description

A schematic model of such a coupled system is shown in Figure 8, where G_i are the subsystems coupled through internal inputs and internal outputs, and y and u are the external output and external input, respectively. The mathematical model in the state space can be either in first-order form,

$$\begin{array}{rcl} E_j \dot{x}_j(t) &=& A_j x_j(t) + B_j u_j(t), \\ y_j(t) &=& C_j x_j(t), \end{array} \tag{17}$$

or in second-order form,

$$\begin{array}{rcl} M_j \ddot{x}_j(t) + E_j \dot{x}_j(t) + K_j x_j(t) &=& B_j u_j(t), \\ y_j(t) &=& C_{j1} \dot{x}_j(t) + C_{j2} x_j(t). \end{array} \tag{18}$$

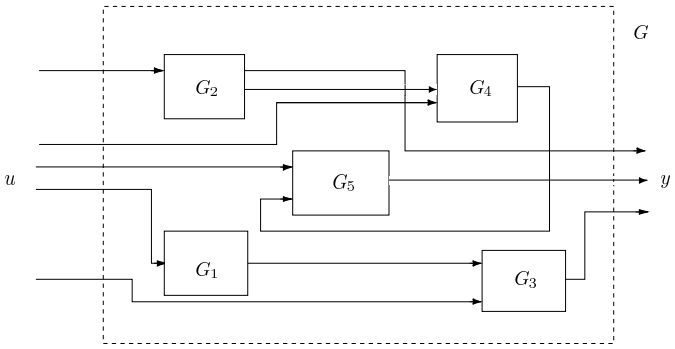

Figure 8: A schematic model of a system coupled through inputs/outputs.

The subsystems in (17) or in (18) are coupled through the relations

$$\begin{aligned} u_j(t) &= D_{j1}y_1(t) + \cdots + D_{jk}y_k(t) + H_j u(t), \quad j = 1, \ldots, k, \\ y(t) &= R_1 y_1(t) + \cdots + R_k y_k(t). \end{aligned} \tag{19}$$

Here $E_j, A_j, M_j, E_j, K_j \in \mathbb{R}^{n_j \times n_j}$, $B_j \in \mathbb{R}^{n_j \times p_j}$, $C_j, C_{j1}, C_{j2} \in \mathbb{R}^{m_j \times n_j}$, $x_j(t) \in \mathbb{R}^{n_j}$ are internal state vectors, $u_j(t) \in \mathbb{R}^{p_j}$ are internal inputs, $y_j(t) \in \mathbb{R}^{m_j}$ are internal outputs, $D_{jl} \in \mathbb{R}^{p_j \times m_l}$, $H_j \in \mathbb{R}^{p_j \times p}$, $R_j \in \mathbb{R}^{m \times m_j}$, $u(t) \in \mathbb{R}^p$ is an external input, and $y(t) \in \mathbb{R}^m$ is an external output. Coupled systems as in (17)–(19) are also called *interconnected* or *composite* systems [28, 33].

As stated in [28], the coupled systems in (17)–(19) may arise from spatial discretization of linear partial differential equations describing physical phenomenons, such as heat transfer, vibrations, electromagnetic radiation or fluid flow, etc.. In simulation of linear RLC circuits that consist of resistors, capacitors, inductors, voltage and current sources only, the corresponding model is of first-order form (17). The components of the state vector $x_j(t)$ are the nodal voltages, the inductor currents and the currents through the voltage sources, $u_j(t)$ contains the currents and voltages of the current and voltage sources, respectively, and $y_j(t)$ consists of the voltages across the current sources and the currents through the voltage sources. Systems of the form in (18) appear also in mechanical and structural dynamics, where $x_j(t)$ is the displacement vector and $u_j(t)$ is the acting force[1].

4.2.2 MOR for interconnected systems

Two approaches are available for MOR of the interconnected system. One is to transform the subsystems into a large closed-loop system and to compute the reduced-order model by any MOR method suitable for linear time invariant systems. The other approach is to compute the reduced-order model of each subsystem, and couple them through the same interconnection relations. In the following, we introduce the two techniques separately.

MOR for a large closed-loop system.

The method is valid for coupled systems in the first-order form in (17). Systems in second-order form as in (18) have to be first transformed into first-order form using the transformation $z_j = \dot{x}_j$, and $\tilde{x}_j = (x_j^T, z_j^T)^T$. In the following, we only consider the system in the first order form (17).

Let $n = n_1 + \cdots + n_k$, $p_0 = p_1 + \cdots + p_k$, and $m_0 = m_1 + \ldots + m_k$. Introducing the matrices

$$R = [R_1, \ldots, R_k] \in \mathbb{R}^{m \times m_0}, \quad H = [H_1^T, \ldots, H_k^T]^T \in \mathbb{R}^{p_0 \times p},$$

and

$$D = [D_{jl}]_{j,l=1}^{k} \in \mathbb{R}^{p_0 \times m_0},$$

together with the block diagonal matrices

$$\begin{aligned} E &= \operatorname{diag}(E_1, \ldots, E_k) \in \mathbb{R}^{n \times n}, \quad A = \operatorname{diag}(A_1, \ldots, A_k) \in \mathbb{R}^{n \times n}, \\ B &= \operatorname{diag}(B_1, \ldots, B_k) \in \mathbb{R}^{n \times p_0}, \quad C = \operatorname{diag}(C_1, \ldots, C_k) \in \mathbb{R}^{m_0 \times n}, \end{aligned}$$

[1] In lack of a better formulation, this subsection is basically copied from [28]

the coupled system in (17) can be rewritten in closed-loop form as

$$\begin{aligned} \mathcal{E}\dot{x}(t) &= \mathcal{A}x(t) + \mathcal{B}u(t), \\ y(t) &= \mathcal{C}x(t), \end{aligned} \tag{20}$$

where the system matrices $\mathcal{E} = E \in \mathbb{R}^{n\times n}, \mathcal{A} = A + BDC \in \mathbb{R}^{n\times n}, \mathcal{B} = BH \in \mathbb{R}^{n\times p}, \mathcal{C} = RC \in \mathbb{R}^{m\times n}$, are of much larger sizes than each of the subsystems.

Model order reduction of the coupled system in (17) is then transformed into model order reduction of the closed-loop system in (20). The closed-loop system is a linear-time invariant system, so that any MOR method which is suitable for such systems can be applied. In [28], the balanced truncation method and the moment-matching method are discussed for MOR of the closed-loop system. For instance, if two projection matrices $W \in \mathbb{R}^{n\times r}$, $V \in \mathbb{R}^{n\times r}$ have been computed by a certain MOR method, the reduced-order model is computed as

$$\begin{aligned} W^T\mathcal{E}V\dot{z}(t) &= W^T\mathcal{A}Vz(t) + W^T\mathcal{B}u(t), \\ \hat{y}(t) &= \mathcal{C}Vz(t). \end{aligned} \tag{21}$$

It is pointed out in [28] that MOR on the closed-loop system ignores the special properties of the subsystems, though the subsystems are usually governed by entirely different physical laws and they often act in different spaces and time scales. Furthermore, the reduced-order model is not flexible in the sense of adding new subsystems, or replacing some of them by new ones, or changing the coupling configuration in the original coupled system. Once the coupled system has undergone the changes above, the reduced-order model has to be re-computed. Furthermore, MOR for the closed-loop system is usually efficient only for systems with a small number of internal inputs and outputs [24].

In Chapter 8 of [24], the generalized singular value decomposition (GSVD) technique is used to get low rank approximations of the coupling blocks in the matrix $\mathcal{A}$ in (20); from the low rank approximations, approximated input and output matrices $\tilde{B}_j$ and $\tilde{C}_j$ that have smaller sizes than the original ones can be extracted. When $\tilde{B}$ and $\tilde{C}$ are used in the moment-matching method to compute the projection matrices W_i, V_i for each subsystem, the size of the reduced-order model can be further reduced. This GSVD technique is shown to be useful for dealing with interconnected systems with many internal inputs and internal outputs.

In the following, a different MOR approach is introduced, where the reduced-order models are separately computed for each of the subsystems. A most suitable model order reduction method can be chosen for each subsystem, by taking the structure and property of the individual subsystem into consideration. The final reduced-order model is obtained by coupling all the reduced-order models for the subsystems through the same coupling relations as the original system.

Separate MOR and then coupling [28].

The advantage of separate MOR and then coupling is that it preserves the structure of the original coupled system in (17). One has the freedom of choosing different MOR methods for different subsystems. The reduced-order model preserves the structure of the original coupled system. Furthermore, parallel computation of the reduced subsystems is possible. The first step of the approach is to apply MOR to each subsystem, and to obtain the reduced subsystems,

$$\begin{aligned} \hat{E}_j\dot{z}_j(t) &= \hat{A}_j z(t) + \hat{B}_j\hat{u}_j(t), \\ \hat{y}_j(t) &= \hat{C}_j z_j(t), \end{aligned} \tag{22}$$

where $\hat{E}_j, \hat{A}_j \in \mathbb{R}^{r_j\times r_j}$. $\hat{B}_j \in \mathbb{R}^{r_j\times p_j}$, $\hat{C}_j \in \mathbb{R}^{m_j\times r_j}$, with $r_j \ll n_j$. The second step consists in coupling the reduced subsystems through the same interconnection relations

$$\begin{aligned} \hat{u}_j(t) &= D_{j1}\hat{y}_1(t) + \cdots + D_{jk}\hat{y}_k(t) + H_j u(t), \quad j = 1, \ldots, k, \\ \hat{y}(t) &= R_1\hat{y}_1(t) + \cdots + R_k\hat{y}_k(t). \end{aligned} \tag{23}$$

Note that the only difference between the coupling in (23) and the coupling for the original system in (19) is that the outputs $y_j(t)$ in (19) are replaced by the approximate outputs $\hat{y}_j(t)$ in (23). Due to the first equation in (23), the input of the reduced subsystem in (22) should be $\hat{u}_j(t)$, rather than $u_j(t)$ in the original system.

To construct the reduced subsystems, various MOR methods could be used. The balanced truncation method and the moment-matching method for MOR of the subsystems are discussed in [15, 24, 28, 29, 33]. When the subsystems are systems of DAEs, they can be first transformed into a system of ordinary differential equations (ODEs) by using ε-embedding techniques [15], and then the moment-matching method is applied to the transformed subsystems. Though relaxing the constraints in DAEs this way is an often employed technique in engineering, it should be noted that this may result in physically questionable results and is numerically hazardous, see, e.g., [18].

5 MOR for nonlinear coupled systems

This section introduces MOR methods for nonlinear coupled systems. Compared to the linear coupled systems in (1) or (2), a nonlinear coupled system has additional nonlinear terms at the positions of $\mathcal{M}$, $\mathcal{E}$, and/or $\mathcal{A}$. In the following sections, we introduce some examples of nonlinear coupled systems. We classify the nonlinear coupled systems into weakly coupled and strongly coupled systems, according to their coupling structure. If the coupling is only a one-way coupling, i.e., if the ith subsystem has a coupling with the jth subsystem, and no coupling exists the other way around, we call it *weak coupling*. Otherwise, we consider it as *strong coupling*.

5.1 Weakly coupled systems

5.1.1 A model of an electro-thermal package.

Weakly coupled systems appear, e.g., from electro-thermal modeling of nano-electronics [5]. See Figure 9 for an electro-thermal package model. For general complex geometries, an accurate physical model in the form of heat transfer partial differential equations is required. The electrical transport is controlled by Ohm's law and the current continuity equation in conductive material is

$$\nabla \cdot \vec{J} = 0, \qquad \vec{J} = \sigma(T)\, \vec{E}, \tag{24}$$

where J (A/m^2) is known as the current density, E (V/m) is the electric field, and σ (1/(Ohm m)) is the conductivity, depending on the temperature T. The generated-energy transport is controlled by Joule's law

$$\frac{\partial U}{\partial t} = -\nabla \cdot \vec{Q} + \Sigma, \qquad \vec{Q} = -\kappa(T)\nabla T, \qquad U = C_V(T - T^*). \tag{25}$$

Of particular interest is the local heat generation, which is given by

$$\Sigma = \vec{E} \cdot \vec{J} = \sigma(T)\,(\nabla V)^2\,. \tag{26}$$

Here, Q (W/m^2) is the heat flux, κ (W/(m K)) is the thermal conductivity, C_V is the constant-volume heat capacitance of the material, which is also T-dependent, and T^* is a reference or ambient temperature. The latter expression results in a non-linear relation (coupling) between the variables V, the electrical voltages, and the temperature variables, T. Spatial discretization (using the finite-element method, or the finite volume method, like finite integration) of (24) and (25) results in a large-scale system of ODEs in the form of

$$\underbrace{\begin{bmatrix} E_{11}(\mu) & 0 \\ 0 & 0 \end{bmatrix}}_{\mathcal{E}(\mu)} \begin{bmatrix} \dot{x}_1 \\ \dot{x}_2 \end{bmatrix} = \underbrace{\begin{bmatrix} A_{11}(\mu) & 0 \\ 0 & A_{22}(\mu) \end{bmatrix}}_{\mathcal{A}(\mu)} \begin{bmatrix} x_1 \\ x_2 \end{bmatrix} + \begin{bmatrix} x_2^T \mathcal{F}(\mu) x_2 \\ 0 \end{bmatrix} + \begin{bmatrix} B_1(\mu) \\ B_2(\mu) \end{bmatrix} u(t), \tag{27}$$

where $x = (x_1^T, x_2^T)^T \in \mathbb{R}^n$ is the state vector including the nodal voltages $x_1 \in \mathbb{R}^{n_1}$ and nodal temperatures $x_2 \in \mathbb{R}^{n_2}$ varying with time. Here, μ is a scalar, describing the variation of the thickness of the top layer of the package. The tensor $\mathcal{F} \in \mathbb{R}^{n_1 \times n_2 \times n_2}$ represents the non-linear character of the heat source Σ. Roughly speaking, $\mathcal{F}$ can be considered as a 3-D array of n_1 matrices $\mathcal{F}_i \in \mathbb{R}^{n_2 \times n_2}$, $i = 1, \ldots, n_1$. As a result, $x_2^T \mathcal{F}(\mu) x_2 \in \mathbb{R}^{n_1}$ represents a vector, where the ith component in the vector is the vector-matrix-vector product $x_2^T \mathcal{F}_i x_2$, for $i = 1, \ldots, n_1$. The matrix $\mathcal{E} \in \mathbb{R}^{n \times n}$ is a capacity matrix for both the electrical and the thermal part, and the matrix $\mathcal{A} \in \mathbb{R}^{n \times n}$ is the conductivity matrix for both the electrical and the thermal part. The coupled system can be very large depending on the number of meshes used for discretization. Model order reduction is required, especially for multi-query simulations due to the variations of μ.

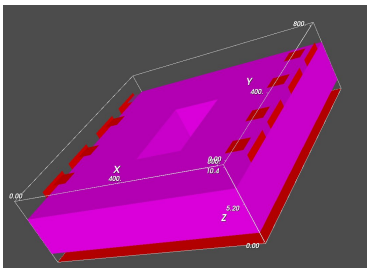

Figure 9: Electro-thermal package. (Courtesy of MAGWEL NV, Leuven (Belgium).)

MOR for the package model.

In the weakly coupled system above, the state vector x_2 acts as an input for the subsystem of x_1. For direct simulation, one can first compute x_2 from the algebraic equation defining x_2, then substitute x_2 into the equation of x_1, to get a subsystem for x_1 without coupling. To achieve fast simulation, MOR can be applied to both the algebraic equation and the subsystem for x_1. In [5], a parametric model order reduction method [4] is used to get a reduced-order model of the algebraic equation in a parametric form, and a parametric reduced-order model of the x_1 subsystem. More specifically, two projection matrices $V_1 \in \mathbb{R}^{n_1 \times r_1}, r_1 \ll n_1$, and $V_2 \in \mathbb{R}^{n_2 \times r_2}, r_2 \ll n_2$, are computed for the two subsystems. When computing V_1, the coupling term $x_2 \mathcal{F} x_2$ is ignored. Nevertheless, it can be used to further improve the accuracy of V_1 if necessary. The reduced-order model of the coupled system is of the form as below,

$$\underbrace{\begin{bmatrix} V_1^T E_{11}(\mu) V_1 & 0 \\ 0 & 0 \end{bmatrix}}_{\hat{\mathcal{E}}(\mu)} \begin{bmatrix} \dot{z}_1 \\ \dot{z}_2 \end{bmatrix} = \underbrace{\begin{bmatrix} V_1^T A_{11}(\mu) V_1 & 0 \\ 0 & V_2^T A_{22}(\mu) V_2 \end{bmatrix}}_{\hat{\mathcal{A}}(\mu)} \begin{bmatrix} z_1 \\ z_2 \end{bmatrix} + \begin{bmatrix} \hat{\mathcal{F}}(\mu, z_2) \\ 0 \end{bmatrix} + \begin{bmatrix} V_1^T B_1(\mu) \\ V_2^T B_2(\mu) \end{bmatrix} u(t), \tag{28}$$

where $\hat{\mathcal{F}}(\mu, z_2) = V_1^T (z_2^T V_2^T \mathcal{F}(\mu) V_2 z_2) \in \mathbb{R}^{r_1}$ is the projected coupled term.

5.2 Strongly coupled systems

5.2.1 An electrical circuit model.

This model comes from modeling of integrated circuits with semiconductor devices [13]. The system is a coupling of a semiconductor model and an RCL system of resistors, capacitors, and inductors, obtained by modified nodal analysis. The RCL system is described by

$$\begin{aligned} \mathcal{E}(x) \tfrac{dx(t)}{dt} &= \mathcal{A}x(t) + f(x(t)) + \mathcal{B}u(t), \\ y &= \mathcal{B}^T x, \end{aligned} \tag{29}$$

where

$$x = \begin{bmatrix} x_1 \\ x_2 \\ x_3 \end{bmatrix}, u = \begin{bmatrix} u_1 \\ u_2 \end{bmatrix},$$

and

$$\begin{gathered} \mathcal{E}(x) = \begin{bmatrix} g_1(x_1) & 0 & 0 \\ 0 & g_2(x_2) & 0 \\ 0 & 0 & 0 \end{bmatrix}, \quad \mathcal{A} = \begin{bmatrix} 0 & A_{12} & A_{13} \\ -A_{12}^T & 0 & 0 \\ -A_{13}^T & 0 & 0 \end{bmatrix}, \\ f(x) = \begin{bmatrix} f_1(x_1) \\ 0 \\ 0 \end{bmatrix}, \quad \mathcal{B} = \begin{bmatrix} B_1 & 0 \\ 0 & 0 \\ 0 & -I \end{bmatrix}. \end{gathered} \tag{30}$$

Here $g_1(x_1) \in \mathbb{R}^{n_1}$, $f_1(x_1) \in \mathbb{R}^{n_1}$ and $g_2(x_2) \in \mathbb{R}^{n_2}$ are nonlinear functions of $x_1 \in \mathbb{R}^{n_1}$ and $x_2 \in \mathbb{R}^{n_2}$, respectively. The system in (29) can be further decoupled into linear and nonlinear parts [13].

The model of the semiconductor is in the following form,

$$\begin{aligned} \tilde{\mathcal{E}}(\tilde{x}) \tfrac{d\tilde{x}(t)}{dt} &= \tilde{\mathcal{A}}\tilde{x}(t) + \tilde{f}(\tilde{x}(t)) + \tilde{b}(x_1), \\ \tilde{y} &= \tilde{g}(x_1), \end{aligned} \tag{31}$$

where

$$\tilde{x} = \begin{bmatrix} \tilde{x}_1 \\ \tilde{x}_2 \\ \tilde{x}_3 \end{bmatrix},$$

and

$$\tilde{\mathcal{E}}(x) = \begin{bmatrix} 0 & 0 & 0 \\ 0 & M & 0 \\ 0 & 0 & 0 \end{bmatrix}, \quad \tilde{f}(\tilde{x}) = \tilde{f}(\tilde{x}_2, \tilde{x}_3). \tag{32}$$

Note that the semiconductor model is coupled with the RCL system through the state vector x_1.

MOR for the coupled circuit model.

In [13], the coupled systems in (29) and (31) are decoupled into linear and nonlinear systems, by making use of the properties of the circuits. The linear system is reduced by the algorithm PABTEC [13]. The nonlinear systems are reduced by the proper orthogonal decomposition (POD) method, combined with discrete interpolation of the nonlinear functions using the Discrete Empirical Interpolation Method (DEIM) [7]. The decoupled subsystems are then replaced by their reduced-order models, which are coupled again to constitute the final coupled reduced-order model. An illustration of the procedure is given in Figure 10. The details of MOR are discussed in [13]. From the simulation results for the circuit example in [13], a speedup factor of 20 by using MOR can be deduced. The dimension of the reduced-order model is 130, while the original coupled system has a size of $n = 7,510$.

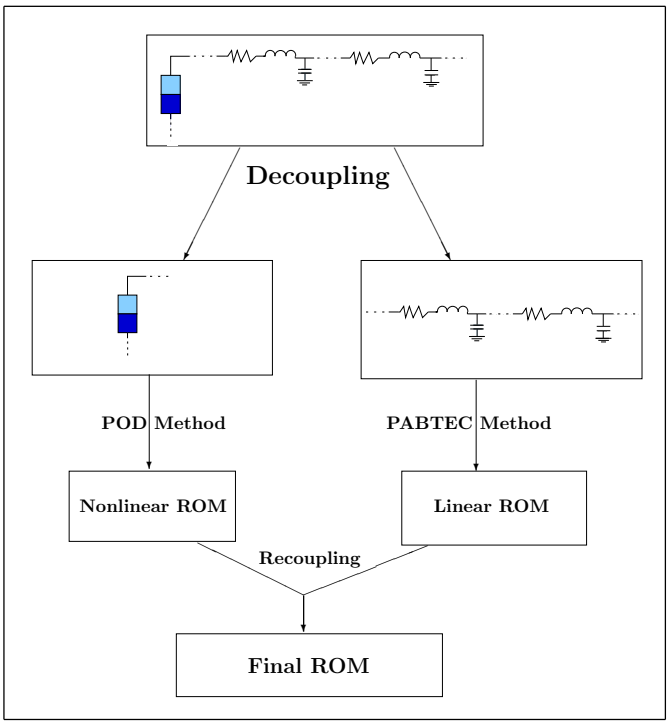

Figure 10: MOR for integrated circuit with semiconductors.

5.2.2 A model of lithium ion batteries.

In [20], a coupled system consisting of two elliptic and one parabolic equations is considered for MOR. The parabolic equation describes the concentration of lithium ions, and the two elliptic equations describe the potential in the solid and liquid phases, respectively. These equations are coupled by a strong nonlinearity, which is a concatenation of the square root, the hyperbolic sine, and the logarithmic functions. Moreover, the system has a vector μ of parameters. In summary, it is a parametric nonlinear coupled system. The coupled system, after finite element discretization (FEM) of the model of PDEs, is given as below,

$$\begin{aligned} M\dot{x}_1(t) + S_1x_1(t) + N(x_1(t), x_2(t), x_3(t); \mu) &= 0 \quad \text{for all } t \in [0, T], \\ x_1(0) &= x_1^0, \ t = 0, \\ S_2x_2(t) + N(x_1(t), x_2(t), x_3(t); \mu) &= 0 \quad \text{for all } t \in [0, T], \\ S_3x_3(t) - N(x_1(t), x_2(t), x_3(t); \mu) &= 0 \quad \text{for all } t \in [0, T], \end{aligned} \tag{33}$$

where $M \in \mathbb{R}^{n\times n}, S_1 \in \mathbb{R}^{n\times n}$, and the nonlinear function $N(\cdot, \mu) \in \mathbb{R}^n$. Here $x_1 \in \mathbb{R}^n$, $x_2 \in \mathbb{R}^n$, and $x_3 \in \mathbb{R}^n$ represent the FEM solutions of the parabolic equation, and two elliptic equations, respectively.

MOR for the model of lithium ion batteries

The POD method is used in [20] to compute the projection matrices $V_1 \in \mathbb{R}^{n\times r_1}, V_2 \in \mathbb{R}^{n\times r_2}, V_3 \in \mathbb{R}^{n\times r_3}, r_1, r_2, r_3 \ll n$ for MOR of the system above. The reduced-order model in (34) is obtained by applying Galerkin projection to

each subsystem in (33), using V_1, V_2, V_3, respectively,

$$\begin{aligned} V_1^T M V_1 \dot{z}_1(t) + V_1^T S_1 V_1 z_1(t) + V_1^T N(V_1 z_1(t), V_2 z_2(t), V_3 z_3(t); \mu) &= 0 \quad \text{for all } t \in [0,T], \\ V_1^T M V_1 z_1(0) &= z_1^0, \\ V_2^T S_2 V_2 z_2(t) + V_2^T N(V_1 z_1(t), V_2 z_2(t), V_3 z_3(t); \mu) &= 0 \quad \text{for all } t \in [0,T], \\ V_3^T S_3 V_3 z_3(t) - V_3^T N(V_1 z_1(t), V_2 z_2(t), V_3 z_3(t); \mu) &= 0 \quad \text{for all } t \in [0,T]. \end{aligned} \tag{34}$$

To accelerate the computation of the nonlinear function $N(\cdot, \mu)$ in the reduced-order model (34), the DEIM algorithm [7] and the Empirical Interpolation Method (EIM) [2] are applied to get an empirical interpolation of $N(\cdot, \mu)$. It is observed that for the test example used for multiple evaluations of the system, the POD method combined with EIM or DEIM is able to speed up the simulation by a factor of 35.

5.2.3 A coupled Schroedinger-Poisson system.

Solving a coupled Schroedinger-Poisson system of equations arises from ballistic transport simulation in nanodevices. In [27], the model of PDEs is described in detail. A subband decomposition approach is combined with the finite element discretization to solve the original system of PDEs. The reduced basis method is applied to construct the reduced-order model, which has significantly reduced the computational cost. Because of the involved formulations, the equations of the model are not presented. It is worth noting that, in general, the reduced basis method relies on a suitable a posteriori error estimation of the reduced-order model to efficiently construct the reduced basis, i.e., the projection matrix for MOR. Usually, the method is suitable for parametric systems. For the examples examined in [27], the reported speedup factor of the reduced basis method is around 2.

5.2.4 A batch chromatographic model.

Batch chromatography, as a crucial separation and purification tool, is widely employed in food, fine chemical and pharmaceutical industries. The principle of batch elution chromatography for binary separation is shown schematically in Figure 11. The governing equations in the dimensionless form are formulated as follows,

$$\begin{cases} \dfrac{\partial c_z}{\partial t} + \dfrac{1-\epsilon}{\epsilon}\dfrac{\partial q_z}{\partial t} = -\dfrac{\partial c_z}{\partial x} + \dfrac{1}{Pe}\dfrac{\partial^2 c_z}{\partial x^2}, & 0 < x < 1, \\ \dfrac{\partial q_z}{\partial t} = \dfrac{L}{Q/(\epsilon A_c)} \kappa_z \left(q_z^{\mathrm{Eq}} - q_z\right), & 0 \le x \le 1, \end{cases} \tag{35}$$

where c_z, q_z are the concentrations of the component $z\,(z = \mathsf{a}, \mathsf{b})$ in the liquid and solid phase, respectively. Here, the four variables c_z, q_z, $z\,(z = \mathsf{a}, \mathsf{b})$ are coupled through the first equation and the adsorption equilibrium $q_z^{\mathrm{Eq}} = f_z(c_\mathsf{a}, c_\mathsf{b})$ in the second equation which can be linear or nonlinear. The coupling is very complex, especially for the nonlinear case. For instance, the following nonlinear case was considered in [35],

$$q_z^{\mathrm{Eq}} = f_z(c_\mathsf{a}, c_\mathsf{b}) := \frac{H_{z1} c_z}{1 + K_{\mathsf{a}1} c_\mathsf{a}^\mathsf{f} c_\mathsf{a} + K_{\mathsf{b}1} c_\mathsf{b}^\mathsf{f} c_\mathsf{b}} + \frac{H_{z2} c_z}{1 + K_{\mathsf{a}2} c_\mathsf{a}^\mathsf{f} c_\mathsf{a} + K_{\mathsf{b}2} c_\mathsf{b}^\mathsf{f} c_\mathsf{b}}. \tag{36}$$

The flow rate Q and the injection period t_{in} (in the boundary conditions) are considered as parameters, i.e., $\mu := (Q, t_{\mathrm{in}})$. Other parameters in the above equations are constants, and details about them can be found in [35]. In short, this is a parametrized nonlinear time-dependent system.

MOR for the batch chromatographic model

In [35], the finite volume discretization is used to construct the discretized full-order coupled model of the PDEs in (35). The reduced basis method is employed to construct the reduced-order models for the discretized models of the variables c_z, q_z, $z = a, b$, separately. The final reduced-order model is obtained by coupling the individual reduced-order models using the same coupling relationship as that in the full-order coupled model. To avoid computing the nonlinear coupled term in the full dimension, it is treated using the EIM algorithm [2]. The resulting reduced-order model preserves the block structure of the full-order coupled model, and is reliable over the whole interesting parameter domain, such that the underlying optimization problem is efficiently solved using the reduced-order model. Solving the optimization problem with the reduced-order model is about 50 times faster than optimization employing the original coupled system.

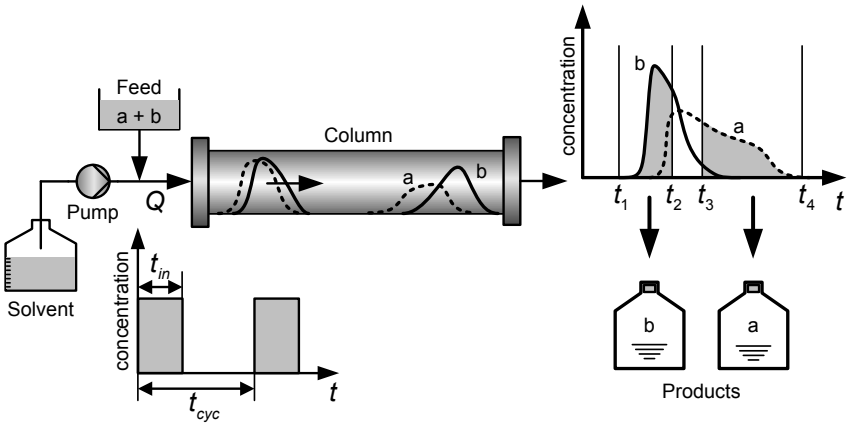

Figure 11: Sketch of a batch chromatographic process for the separation of a and b.

5.2.5 Simulated moving bed (SMB) chromatography model

Simulated moving bed (SMB) chromatography is a continuous multi-column process and has been widely used as an efficient separation technique in chemical industries. An SMB unit usually consists of several identical chromatographic columns connected in a series, see Figure 12. The governing equations for the fluid flow in each chromatographic column is similar to that of the batch chromatographic model, and some balance equations are used to describe the relations of the flow between the inlet and outlet ports of two successive columns. This system is a multi-stage system driven by a periodic switching procedure, namely, a final cyclic steady state is achieved usually through cycle by cycle simulations.

MOR for the SMB chromatography

Several MOR methods have been applied to the SMB chromatography, see [21, 22, 36], for example.

In [21], the SMB model of PDEs is discretized using orthogonal collocation on finite elements (OCFE), and the discretized system is written as:

$$M\dot{x}(t) = A(\mu)x(t) + B(\mu) + F(x(t), \mu), \quad t \in [0, 1], \tag{37}$$

where $x \in \mathbb{R}^n$ is the state vector that represents the concentrations in the liquid and solid phases at the grid nodes, $M \in \mathbb{R}^{n\times n}$, $A \in \mathbb{R}^{n\times n}$, $B \in \mathbb{R}^n$ are the coefficient matrices, and $F(\cdot) \in \mathbb{R}^n$ is a nonlinear vector-valued function, describing the coupling of the systems. Here the parameters of the system in (37) are the dimensionless time t, and the vector $\mu \in \mathbb{R}^q$ of the operating conditions.

The POD method is applied to a nonlinear SMB model in [21]. An efficient Krylov-subspace MOR method is proposed for a linear SMB model in [22]. The reduced-order models are built without considering the block structure of the original coupled system, and hence are dense.

More recently, the reduced basis method was applied to a linear SMB model in [36]. The finite volume method is used to construct the discretized full-order coupled model. The reduced-order model for each variable is computed in a separate way, and then they are coupled with the same relation as the original full-order model. The resulting reduced-order model, therefore, preserves the block structure of the full-order coupled model. The reduced-order model is then applied within an optimization problem to obtain the optimal operating conditions of SMB. The optimization has been accomplished with acceptable accuracy, but with much less time, and the speedup factor is 9 as compared to standard optimization with the original coupled system.

6 Conclusions

We have reviewed MOR methods for different coupled systems with various application backgrounds. The coupled systems can be linear or nonlinear, and sometimes also include symbolic parameters. For linear coupled systems, the MOR methods used are usually balanced truncation, moment-matching, though MOR methods based on eigenmodes of the system are usually used in the area of structural dynamics. For nonlinear systems, the most commonly used methods are POD if the system is strongly nonlinear, and methods based on Krylov subspaces

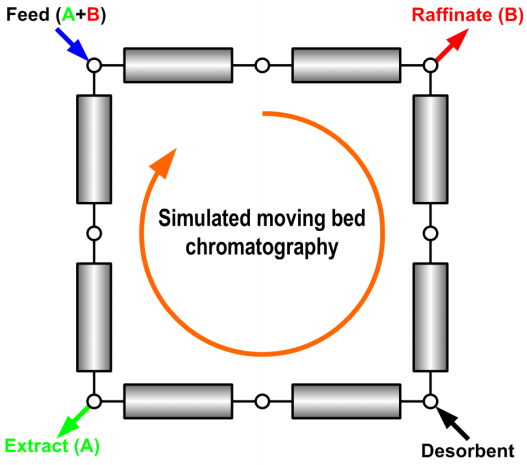

Figure 12: Schematic illustration of an SMB chromatographic process with four zones and eight columns.

(e.g., moment-matching) could be applied for weakly nonlinear (e.g., quadratic) systems. For parametric systems, reduced basis methods are popular, especially for MOR of nonlinear parametric systems, whereas the Krylov subspace based methods (e.g., multi-moment-matching) are efficient for dealing with linear parametric systems. Certainly, this survey is not exhaustive, and the list of coupled problems discussed here is certainly incomplete. Nevertheless, we hope to have provided a good starting point for further research in MOR for coupled problems.

Acknowledgments

This work was supported by the Robert Bosch GmbH Stuttgart, Projekt ARH-243 “Nichtlineare Modellordungsreduktion von Navier-Stokes Gleichungen mit dem QBDAE Ansatz”, and the collaborative project nanoCOPS: “Nanoelectronic COupled Problems Solutions”, supported by the European Union in the FP7-ICT-2013-11 Program under Grant Agreement Number 619166.

We thank Norman Lang, Mohammed Monir Uddin, and Yongjin Zhang of the Max Planck Institute, Magdeburg, for providing some of the models presented in Section 4.1 and Section 5.2.

References

[1] A.C. Antoulas and D.C. Sorensen. Approximation of large-scale dynamical systems: an overview. *International Journal of Applied Mathematics and Computer Science*, 11(5):1093–1121, 2001.

[2] M. Barrault, Y. Maday, N.C. Nguyen, and A. T. Patera. An ‘empirical interpolation’ method: Application to efficient reduced-basis discretization of partial differential equations, C. R. Acad. Sci. Paris Ser. I, 339: 667–672, 2004.

[3] U. Baur, C. A. Beattie, P. Benner and S. Gugercin. Interpolatory Projection Methods for Parameterized Model Reduction. *SIAM Journal on Scientific Computing*, 33(5):2489–2518, 2011.

[4] P. Benner and L. Feng. A robust algorithm for parametric model order reduction based on implicit moment matching. *In: A. Quarteroni, G. Rozza (eds.): Reduced Order Methods for modeling and computational reduction, MS &A 9*, 159–185. Springer International Publishing Switzerland, 2014.

[5] P. Benner, L. Feng, W. Schoenmaker and P. Meuris. Parametric modeling and model order reduction of coupled problems. *ECMI Newsletter*, 68–69, 2014. Available from http://www.mafy.lut.fi/EcmiNL/issues.php.

[6] P. Benner, J. Saak, and M. M. Uddin. Second order to second order balancing for index-1 vibrational systems. *Proceedings of 7th International Conference on Electrical and Computer Engineering*, IEEE, 933–936, 2012.

[7] S. Chaturantabut and D. C. Sorensen. Nonlinear model reduction via discrete empirical interpolation. *SIAM Journal on Scientific Computing*, 32(5):2737–2764, 2010.

[8] R. R. Craig, Jr. Coupling of substructures for dynamic analyses: an overview. *AIAA Journal*, 2000-1573, 2000.

[9] E. J. Davison. A method for simplifying linear dynamic systems. *IEEE Transactions on Automatic Control*, 11(1):93–101, 1966.

[10] M. R. Eslami, R. B. Hetnarski, J. Ignaczak, N. Noda, N. Sumi, and Y. Tanigawa. Theory of Elasticity and Thermal Stresses, Springer, Dordrecht, 2013.

[11] F. D. Freitas, J. Rommes, and N. Martins. Gramian-based reduction method applied to large sparse power system descriptor models *IEEE Transactions on Power Systems*, 23(3):1258–1270, 2008.

[12] E. J. Grimme. Krylov projection methods for model reduction. PhD thesis, University of Illinois at Urbana-Champaign, 1997.

[13] M. Hinze, M. Kunkel, and A. Steinbrecher, T. Stykel. Model order reduction of coupled circuit-device systems. *International Journal of Numerical Modeling: Electronic Networks, Devices and Fields*, 25:362–377, 2012.

[14] W. C. Hurty. Vibrations of structural systems by component-mode synthesis. *Journal of the Engineering Mechanics Division (ASCE)*, 86:51–69, 1960.

[15] Y. L. Jiang, C.Y. Chen, and H.B. Chen. Model-order reduction of coupled DAE systems via ε-embedding technique and Krylov subspace method. *Journal of Franklin Institute*, 349:3027–3045, 2012.

[16] P. Koutsovasilis and M. Beitelschmidt. Comparison of model reduction techniques for large mechanical systems A study on an elastic rod. *Multibody System Dynamics*, 20:111–128, 2008.

[17] B. Kranz. Zustandsraumbeschreibung von piezo-mechanischen Systemen auf Grundlage einer Finite-Elemente-Diskretisierung. *In: ANSYS Conference & 27th CADFEM Users' Meeting 2009.*, 2009. Available from http://publica.fraunhofer.de/documents/N-114493.html.

[18] P. Kunkel and V. Mehrmann. Differential-Algebraic Equations Analysis and Numerical Solution. EMS Publishing House, Zuerich, Switzerland, 2006.

[19] N. Lang, J. Saak, and P. Benner. Model Order Reduction for Systems with Moving Loads. *at-Automatisierungstechnik*, 62(7):512–522, 2014.

[20] O. Lass and S. Volkwein. POD Galerkin schemes for nonlinear elliptic-parabolic systems. *SIAM Journal on Scientific Computing*, 35(3):A1271–A1298, 2013.

[21] S. Li, L. Feng, P. Benner, and A. Seidel-Morgenstern. Using surrogate models for efficient optimization of simulated moving bed chromatography. *Computers & Chemical Engineering*, 67:121–132, 2014.

[22] S. Li, Y. Yue, L. Feng, P. Benner, and A. Seidel-Morgenstern. Model reduction for linear simulated moving bed chromatography systems using Krylov-subspace methods. *AIChE Journal*, 60(11):3773–3783, 2014.

[23] B. S. Liao, Z. Bai, and W. Gao. The important modes of subsystems: A moment-matching approach. *International Journal for Numerical Methods in Engineering*, 70:1581–1597, 2007.

[24] A. Lutowska. Model order reduction for coupled systems using low-rank approximations. *PhD thesis*, Department of Mathematics and Computer Science, Eindhoven University of Technology, Eindhoven, The Netherlands, 2012.

[25] I. Martini, G. Rozza, and B. Haasdonk. Reduced basis approximation and a-posteriori error estimation for the coupled Stokes-Darcy system. *Advances in Computational Mathematics*, 2014. DOI:10.1007/s10444-014-9396-6.

[26] R. Neugebauer, K. Pagel, A. Bucht, V. Wittstock, and A. Pappe. Control concept for piezo-based actuator-sensor-units for uniaxial vibration damping in machine tools. *Production Engineering*, 4:413–419, 2010.

[27] G. S. H. Pau. Reduced basis method for simulation of nanodevices. *Physical Review B*, 78, 155425, 2008.

[28] T. Reis and T. Stykel. A survey on model reduction of coupled systems. *In Model Order Reduction: Theory, Research Aspects and Applications (eds: W. Schilders, H.A. Van der Vorst, J. Rommes)* Mathematics in Industry, Springer, 13:133–155, 2008.

[29] T. Reis and T. Stykel. Stability analysis and model order reduction of coupled systems. *Mathematical and Computer Modelling of Dynamical Systems*, 13(5):413–436, 2007.

[30] B. B. Smida, R. Majed, N. Bouhaddi, and M. Ouisse. Investigations for a model reduction technique of fluid-structure coupled systems. *Proceedings of IMechE vol. 226 Part C: J. Mechanical Engineering Science*, 42-54, 2011.

[31] T. Stykel. Gramian-based model reduction for descriptor systems. *Mathematics of Control, Signals, and Systems*, 16(4):297–319, 2004.

[32] M. M. Uddin, J. Saak, B. Kranz, and P. Benner. Computation of a compact state space model for an adaptive spindle head configuration with piezo actuators using balanced truncation. *Production Engineering*, 6 (6):577–586, 2012.

[33] A. Vandendorpe and P. Van Dooren. Model reduction of interconnected systems. *In Model Order Reduction: Theory, Research Aspects and Applications (eds: W. Schilders, H. A. Van der Vorst, J. Rommes)* Mathematics in Industry, Springer, 13:305–321, 2008.

[34] J. F. Villena, W. H. A. Schilders, and L. M. Silveira. Order reduction techniques for coupled multi-domain electromagnetic based models. *Proceedings of Computational Methods for Coupled Problems in Science and Engineering*, 1–11, 2009.

[35] Y. Zhang, L. Feng, S. Li, and P. Benner. Accelerating PDE constrained optimization by the reduced basis method: application to batch chromatography. *Max Planck Institute Magdeburg Preprint MPIMD/14-09*, 2014. Available from http://www.mpi-magdeburg.mpg.de/preprints/.

[36] Y. Zhang, L. Feng, S. Li, and P. Benner. An efficient output error bound for model order reduction of parametrized evolution equations. *Max Planck Institute Magdeburg Preprint MPIMD/14-22*, 2014. Available from http://www.mpi-magdeburg.mpg.de/preprints/.